

Two Dimensional Mechanism for Insect Hovering

Z. Jane Wang*

Theoretical and Applied Mechanics, Cornell University, Ithaca, New York 14853

(Received 3 May 2000)

Resolved computation of two dimensional insect hovering shows for the first time that a two dimensional hovering motion can generate enough lift to support a typical insect weight. The computation reveals a two dimensional mechanism of creating a downward dipole jet of counterrotating vortices, which are formed from leading and trailing edge vortices. The vortex dynamics further elucidates the role of the phase relation between the wing translation and rotation in lift generation and explains why the instantaneous forces can reach a periodic state after only a few strokes. The model predicts the lower limits in Reynolds number and amplitude above which the averaged forces are sufficient.

PACS numbers: 87.19.St, 47.11.+j, 47.32.Cc

A central question in hovering insect flight is how does an insect generate enough lift to keep it aloft. Early quasisteady analysis failed to predict sufficient force required for hovering, hence the myth “bumblebees cannot fly according to conventional aerodynamics.” This led to the recognition that unsteady effects must be important [1,2]. On the surface, the myth about insect flight is a nuisance leftover from history. No one doubts that insects can fly, nor does one doubt that flow around an insect wing obeys the Navier-Stokes equation. However because the resolution of the myth hinges on our understanding of unsteady flows interacting with dynamic boundaries, a notoriously difficult problem in fluid dynamics, the myth has not been put to rest after more than 50 years. The difficulties include quantifying unsteady effects and identifying a minimal model which contains the essence of hovering flight.

Recently, several elegant experiments of robotic insect wings made significant advances in quantifying some of the unsteady effects. In particular, Ellington *et al.* observed a coherent three dimensional leading-edge vortex that could enhance the lift, and they argued that three dimensional effects were important for hovering [3]. Dickinson *et al.* measured the unsteady forces on a robotic fruit fly wing and demonstrated the role of wing rotation in force generation [4].

Unlike fixed-wing airplanes, insects fly in a sea of vortices created by their flapping wings. Insects depend on vortices to keep them aloft, especially when they are hovering. Therefore, an important key for solving the mystery of insect flight is the understanding of the vortex shedding due to a rapidly oscillating wing at the intermediate Reynolds numbers, for which no simple theory exists. Although there were many visualization studies of streak lines around an insect wing, the spatial and temporal resolutions were typically inadequate to quantify the vortex dynamics. Theoretically, to quantify flow separation requires solving the Navier-Stokes equation coupled to a dynamic boundary. Part of our challenge is to resolve the highly unsteady vortices shed from thin tips. Previously, a handful of computations aimed to capture qualitative features

of vortex dynamics that were comparable to experiments [5,6]. However, in order to probe the detailed vortex dynamics and predict the forces, improved computation is required. To this end, we developed a high order numerical tool to solve the Navier-Stokes equation around a two dimensional moving wing, which mimics insect flight [7].

Real insect flight, like real airplane flight, is naturally three dimensional. While it is well understood that, to the leading order, lift on an airplane wing can be explained by a two dimensional wing theory, surprisingly little has been explored to determine whether there is a fundamental two dimensional mechanism for insect hovering flight.

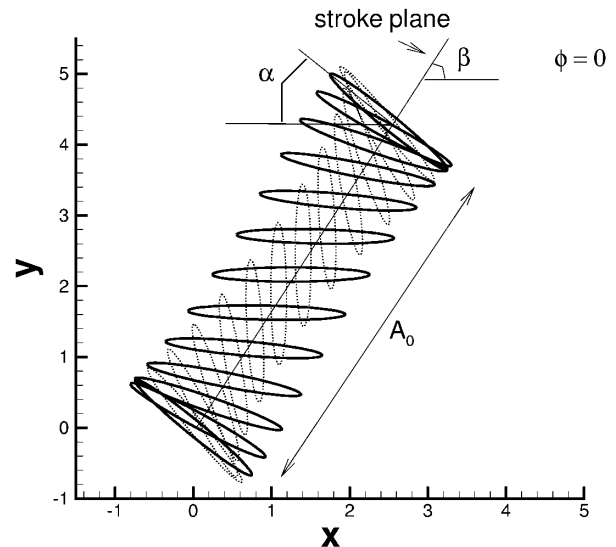


FIG. 1. The positions of a wing element in one period as modeled here. The downstroke phase is indicated by the solid ellipses and the upstroke by the dashed ellipses. The center of the wing is governed by $A(t) = \frac{A_0}{2}[\cos(2\pi t/T) + 1]$, and the angle of attack $\alpha(t) = \pi/4 - \pi/4 \sin(2\pi t/T + \phi)$, where ϕ is the phase difference. The stroke plane is inclined at an angle β . In this study, we pick parameters based on dragonfly data, $A_0 = 2.5$ cm, $T = 0.025$ s, $\beta = \pi/3$, and the chord $c = 1$ cm [9]. The air density and viscosity are $\rho_{\text{air}} = 1.225 \times 10^{-3}$ g/cm³, and $\nu = 0.15$ cm²/s, respectively.

The goal of this work is to quantify the vortex dynamics that is essential for hovering and identify a minimal two dimensional model that produces sufficient lift.

The majority of insects, including dragonflies, hawk-moths, and fruit flies, employ a superposition of heaving and pitching motion to hover, sometimes referred to as a “figure-eight” motion [8]. Figure 1 illustrates a generic sinusoidal motion of an elliptic wing cross-section in the chord direction.

To simulate flow around a hovering wing, we solve the Navier-Stokes equation in elliptic coordinates, (μ, θ) , whose mesh points are naturally clustered around the tips and the body of the ellipse to resolve the boundary layer. The two dimensional Navier-Stokes equation for vorticity has the following form in (μ, θ) :

$$\frac{\partial(S\omega)}{\partial t} + (\sqrt{S}\mathbf{u} \cdot \nabla)\omega = \nu\Delta\omega, \tag{1}$$

$$\nabla \cdot (\sqrt{S}\mathbf{u}) = 0, \tag{2}$$

where \mathbf{u} is the velocity field, ω is the vorticity field, and S is the scaling factor $S(\mu, \theta) = \cosh^2\mu - \cos^2\theta$.

The equation is solved by an explicit fourth-order compact finite difference scheme [7,10]. An advantage of the scheme is that at each time step, only two Poisson solvers are required to achieve a fourth-order spatial accuracy. In addition, the vorticity boundary condition is explicitly enforced. The code was tested against experiments of flow past a cylinder by comparing the velocity field, the separation angle of the shed vortex, and the lift forces [7]. The numerical convergence study shows the accuracy of the code to be fourth order [7]. The time step is chosen such that the change in vorticity is less than 10^{-6} when the time step is reduced to half.

The figure-eight motion turns out to solve two problems simultaneously: to create a dipole and to get rid of it. Figure 2 shows the snapshots of the computed vorticity field near the wing during one period. The wing translation creates a pair of leading and trailing edge vortices of opposite rotation. The wing rotation then combines them into a dipole. Because each vortex induces a flow on the other one, they form a comoving dipole pair. If the timing is correct, such as in this case, where $\phi = 0$, the dipole moves downward carrying momentum with it to generate a lift on the wing. The self-induced flow sweeps away the vortices from the wing, so they do not interfere with the vortices in the next cycle. The shedding frequency in this case is the same as the flapping frequency.

The above mechanism immediately suggests that three dimensionality is not essential for hovering. Previously it was assumed the dipole vortices were formed from the shedding of tip vortices [11,12]—a three dimensional effect. But apparently the figure-eight motion alone can generate a downward flow.

Despite the differences, we observe similarities between the dynamics of vortices in two and three dimensions. In particular, the dominant leading-edge vortex is attached to

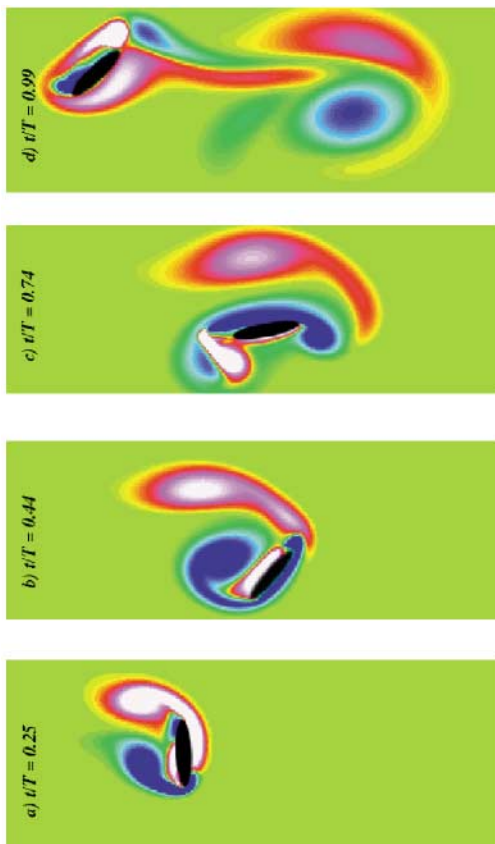


FIG. 2 (color). Snapshots of the vorticity field illustrate the formation and dynamics of a dipole jet during hovering. During the downstroke, as shown in (a) and (b), a pair of counterrotating vortices is generated by the translational motion, and during the upstroke, as shown in (c) and (d), the rotation fuses the leading and trailing edge vortices to form a comoving dipole pair. The dipole and wing then separate in the upstroke phase. At the end of the upstroke, shown in (d), the wing is sufficiently far away from the strong vortices generated in the previous cycle and is ready to repeat the whole process without interfering with the previous vortices. The left vortex rotates clockwise and the right vortex rotates counterclockwise. The parameters are $A = 2.5$ cm, $T = 0.025$ s, $\beta = \pi/3$, $\phi = 0$, $\nu = 2.0$ cm²/s; thus $Re = 157$.

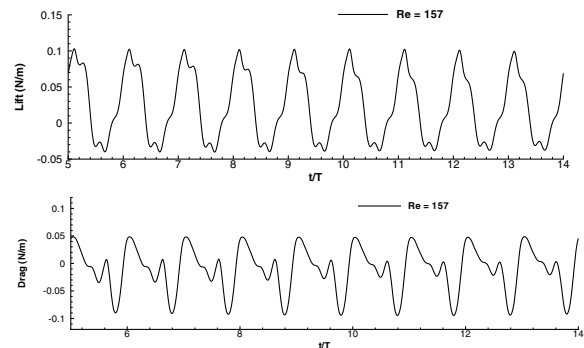


FIG. 3. Time dependent lift and drag per unit span. The time is normalized by its period, 0.025 s.

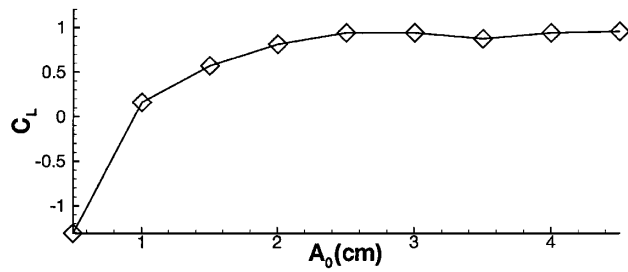


FIG. 4. The lift coefficient (C_L), defined as the lift normalized by $0.5\rho_{\text{air}}cU_{\text{max}}^2$, as a function of normalized amplitude, where U_{max} is the peak value of the translational velocity and c is the chord length.

the wing during the downward phase, which is consistent with experiments [3]. The “dynamic stall” is present in two dimensional hovering partly because the vortex separation time scale is larger than half of the flapping period and partly because the wing rotates.

To quantify the lift and compare it with the weight of a typical insect, we plot the instantaneous forces in Fig. 3. Because ultimately we are interested in the average forces, lift and drag are defined in the vertical (Y) and horizontal (X) direction.

The instantaneous forces reach a nearly periodic state after only a few strokes. It is not *a priori* that an arbitrary periodic wing motion coupled to fluid will immediately generate a periodic force because of the complicated interaction with fluids. In our case, the forces quickly reach an almost periodic state because of negligible interference from vortices generated in previous cycles as seen in Fig. 2, which happens only when rotation and translation are phased correctly. The quick transient to a periodic state in principle enables an insect to take off in a few strokes.

The double peaks in up- and downstrokes resemble typical experimental measurements [4,13]. The averaged two dimensional lift and thrust per unit span over 50 periods are 2.8×10^{-2} and 5.2×10^{-3} N/m, respectively. Repeated computation with twice the spatial resolution gives the same answer in the significant digits.

Based on these values, we estimate the forces on a three dimensional wing using a standard elliptical loading along the wing span [14]. For a wing 5 cm long and 1 cm wide at midspan, we find the total lift supported by one wing is 1.1×10^{-3} N. It follows that two pairs of wings can support 4.4×10^{-3} N, which is more than the weight of a typical dragonfly ranging between 1×10^{-3} to 2.5×10^{-3} N [9]. Three dimensional effects could reduce these computed forces, and the exact factor will be determined in future computation.

To show that these results are not fortuitous, we vary separately the phase, the viscosity, and the amplitude, to study their effects on the forces. Figure 2 suggests that the coupling between translation and rotation is crucial in controlling the formation of the dipole and hence the

TABLE I. Dependence of lift on viscosity ν for the case of $A = 2.5$ cm.

Re	ν (cm ² /s)	Lift per unit span (10^{-2} N/m)
15.7	2.0	1.1
157	0.2	2.8
314	0.1	2.6
628	0.05	2.6
1256	0.025	2.6

lift. To verify this, we repeat the calculation that produced Fig. 2 assuming $\phi = \pi/5$ instead of $\phi = 0$. The average lift and drag are then -1.6×10^{-3} and 1.4×10^{-3} N/m, respectively, which are an order of magnitude smaller than the previous case. Also the “lift” is downward. The sensitivity to ϕ was also reported in the previous experiments [4].

We assume $\phi = 0$ in the remaining studies. Table I shows the average lift and drag for different viscosities. The average force is insensitive to viscosity at sufficiently small viscosities, when $\text{Re} > 157$ in our case, because the lift is dominated by the dynamic pressure rather than by viscous force. These numbers also suggest a low cutoff in Reynolds number, $\text{Re} \sim 15$, when the dragonfly can no longer support its weight by pitching and heaving motion.

Finally lift increases with amplitude almost quadratically as shown by the plateau at a value close to 1 in the lift coefficient plotted in Table I. Again using the typical weight of a dragonfly as a reference point, we predict that the lift is sufficient when $A_0 > 1.5$ cm.

In the light of these findings, we suggest that the two dimensional mechanism for creating a dipole jet discussed here is the leading order mechanism of lift generation in hovering flight employing figure-eight strokes. We expect that in three dimensions, a two dimensional slice in the chord direction has a qualitatively similar structure as that depicted in Fig. 2. Although our model neglects many details, the fact that sufficient lift can be generated from a generic hovering motion suggests that additional effects for lift enhancement are refinements rather than necessities.

I am grateful to Steve Childress and Mike Shelley for advice and useful discussions and to Steve Strogatz and Andy Ruina for critiques of the final version of the manuscript. The work was partly supported by NSF Grant No. DMS-9510356 and DOE Grant No. DE-FG02-88ER25053 through Courant Institute of Mathematical Sciences of New York University.

*Email address: jane.wang@cornell.edu

[1] T. Weis-Fogh and M. Jensen, Proc. R. Soc. London B **239**, 415 (1956); see also reviews by T. Maxworthy, Annu. Rev. Fluid Mech. **13**, 329 (1981); G.R. Spedding, Contemp. Math. **141**, 401 (1993); R. Dudley, *The*

- Biomechanics of Insect Flight* (Princeton University Press, Princeton, 2000).
- [2] C. P. Ellington, *Philos. Trans. R. Soc. London B* **305**, 1 (1984).
- [3] C. P. Ellington, C. van den Berg, A. P. Willmott, and A. L. R. Thomas, *Nature (London)* **384**, 626 (1996).
- [4] M. H. Dickinson, F. O. Lehmann, and S. P. Sane, *Science* **284**, 1954 (1999).
- [5] P. Freymuth, K. Gustavson, and R. Leben, in *Vortex Method and Vortex Motion*, edited by K. Gustavson and J. Sethian (SIAM, Philadelphia, 1991), p. 143.
- [6] H. Liu, C. Ellington, K. Kawachi, C. van den Berg, and A. P. Willmott, *J. Exp. Biol.* **201**, 461 (1998).
- [7] Z. J. Wang, *J. Fluid Mech.* **410**, 323 (2000).
- [8] An exception is a special class of tiny insects; see T. Weis-Fogh, *J. Exp. Biol.* **59**, 169 (1973); M. J. Lighthill, *J. Fluid Mech.* **60**, 1 (1973).
- [9] J. M. Wakeling and C. P. Ellington, *J. Exp. Biol.* **200**, 557 (1997); S. Savage, B. G. Newman, and D. T.-M. Wong, *J. Exp. Biol.* **83**, 59 (1979).
- [10] W. E and J.-G. Liu, *J. Comput. Phys.* **126**, 122 (1996).
- [11] J. Rayner, *J. Fluid Mech.* **91**, 697 (1979).
- [12] M. J. Lighthill, *Mathematical Biofluidynamics* (SIAM, Philadelphia, 1975).
- [13] M. Cloupeau, J. F. Devillers, and D. Devezeaux, *J. Exp. Biol.* **80**, 1 (1979).
- [14] A. M. Kuethe and C.-Y. Chow, *Foundations of Aerodynamics* (John Wiley & Sons, New York, 1976).